Permanent Magnet Synchronous Machines with Improved Energetic Performances and Reduced Torque Ripples, used for Electric Vehicles

D. Fodorean*, *Member*, *IEEE*, F. Jurca*, *Member*, *IEEE*, C. Oprea* and L. Szabo*, *Member*, *IEEE*
* Technical University of Cluj-Napoca, Center of Applied Researches in Electrical Engineering and Sustainable Development; Address: Memorandumului 28, Cluj-Napoca, 400114, Cluj (*Romania*)

***Abstract*-- The paper presents the study of two permanent magnet synchronous machines, with outer rotor, dedicated for electric scooter applications. The electrical machines will be analyzed in order to assure the most suited scooter propulsion. The variety of topology is basically obtained through specific winding configuration and poles/slots ratio. The design results are validated numerically through finite element method. A skewed topology proves the reduction of torque ripples. Also, in order to improve the energetic performances of the studied machines, a unity power-factor control strategy is employed.**

***Index Terms*—permanent magnet synchronous machine, improved energetic performances, electric vehicle.**

I. Introduction

In our days, practically, each automobile constructor proposes alternative solutions to the thermal vehicle: with different degrees of hybridization (from the motorization or supplying point of view) or pure electric automobiles. There are several international conventions which state the future trends in the automobile market [1], [2], [3]. One of these programs called SUPERCAR, [1], imposes the pollution level as a target which should be reached by future automobiles. This task supposes that every element of the automobile needs to be efficiently optimized, to fulfill the final goal. The propulsion system, on a hybrid-electric automobile, can be presented like in Fig. 1. Here, one can distinguish:

- the supplying part (ultracapacitors and battery – which gave the hybrid character of the application);
- the control part (the static converter and the control unit - not shown here);

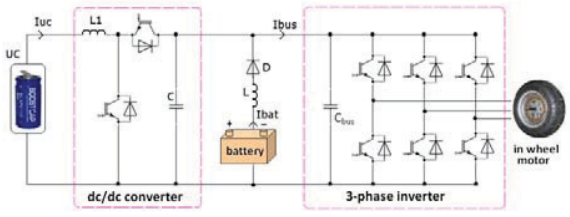

Fig. 1. Electric circuit layout for the studied hybrid-electric scooter.

This paper was supported by the project "Development and support of multidisciplinary postdoctoral programmes in major technical areas of national strategy of Research - Development - Innovation" 4D-POSTDOC, contract no. POSDRU/89/1.5/S/52603, project co-funded by the European Social Fund through Sectoral Operational Programme Human Resources Development 2007-2013.

- the electrical machine (in-wheel configuration, for scooter application in this case).

The research work presented here concerns the study of a hybrid-electric scooter which is intended to have an improved autonomy. It is true that one of the biggest problems of the electric automobile is related to the reduced autonomy offered by the battery and the important time to refill it. On the other hand, in order to reduce the electric power consumption from the battery, it is needed to optimize the element which absorbs the current: the electrical machine [4], [5]. Thus, the paper presents two permanent magnet synchronous machines (PMSM) topologies with different winding configurations and poles/slots ratio, and with a skewing factor. A special attention will be paid to the energetic performances of the machine, by means of improved power factor and decreased torque ripples.

II. Studied Electrical Machines

There are two variants for placing the electrical machine on a scooter:

- by using a classical electrical motor (with inner rotor) [6] with a traction belt, or,
- to use a wheel motor (with outer diameter), [3].

Here, the 2nd variant will be employed.

In order to improve the electrical machines performances, several winding topologies will be analyzed. The output performances of the studied motors are: 1500 W output power, 420 r/min rated speed and 48 Vcc voltage.

The 1st studied topology is based on an outer rotor PMSM, having 9 poles and a distributed winding placed on 54 slots. In order to reduce the torque ripples, an important number of poles or slots should be used. Even if frequency is increased due to high number of poles, for low speed applications, the use of high number of poles and slots is the best way to reduce: the volume of the machine, the torque ripples, and finally vibrations due to electromagnetic causes. This configuration will be called PMSM-9/54, Fig.2a.

The 2nd studied variant is with 23 pair of poles and 51 slots, called PMSM-23/51, Fig. 2b. This variant should produce very smooth induced electromotive force (*emf*), as well as a smooth torque wave. Because of high frequency, there might be some extra iron loss - this should be verified numerically.

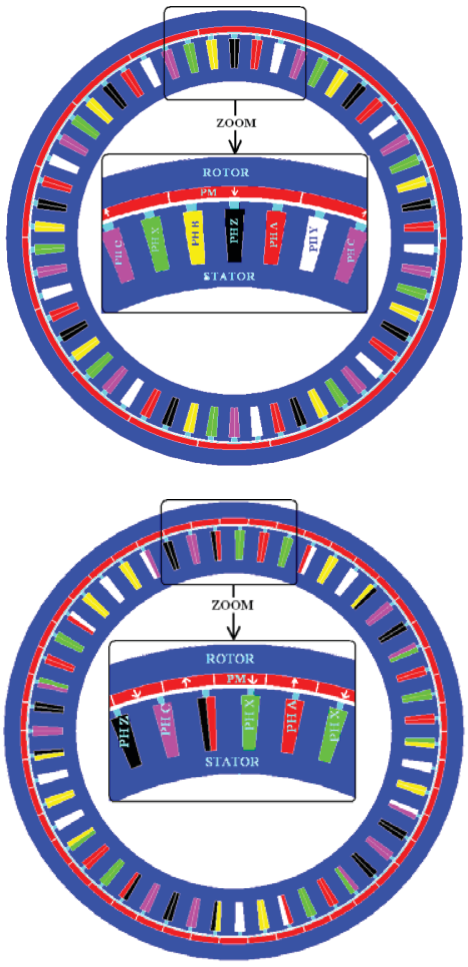

Fig. 2. Studied electrical machines variants: (a) PMSM-9/54; (b) PMSM-23/51.

The design of the machine is based on magnetic reluctance equivalent circuit, [7].

The obtained results are summarized in Table I.

TABLE I
COMPARISON OF OBTAINED RESULTS AFTER THE DESIGN PROCESS OF STUDIED MACHINES

parameter	PMSM-9/54	PMSM-23/51
Rated torque (N·m)	34	
Number of phases (-)	3	3
Number of pole pairs (-)	9	23
Frequency (Hz)	63	161
Number of slots (-)	54	51
Outer diameter (mm)	223	223
Stack length (mm)	50	50
Airgap length (mm)	1	1
Airgap flux density (T)	0.828	0.843
Phase resistance (Ω)	0.073268	0.059563
d, *q* inductances (mH)	0.60011	0.14755
emf (V)	24.65	24.40
Rated current (A)	21.32	24.78
Total losses (W)	136.2	152.4
Power factor (%)	92.27	80.19
Efficiency (%)	91.67	90.77
Active part costs (€)	79.34	80.20
Active part mass (kg)	6.45	6.73
Power/mass ratio (W/kg)	232.2	222.8

In order to decide which machine could offer better results, one should inspect the following parameters: current consumption, total losses, efficiency and power factor, power/mass ratio. It can be observed that the obtained results are very closed, for both machines. In order to decide which variant will provide better performances, we will consider supplementary results from numerical computation.

III. NUMERICAL VALIDATION OF THE STUDIED PMSM

The numerical computation is used to validate the analytical approach. This analysis consists in the computation of the electromagnetic field of electrical machines via the finite element method (FEM). Several parameters will be verified from FEM analysis: the flux density in the air-gap, the torque for rated current supply, *emf* and iron loss. Both, generator and motor operation regimes will be verified on the studied PMSM.

For traction applications, the load varies rapidly and in high intervals. A speed control is, therefore, not suited in this case. Instead, a torque control technique should be employed. In order to have a good torque control, a very smooth torque wave form is needed. Thus, another criterion for choosing the best PMSM variant will be the torque wave form – with reduced torque ripples.

The results from the FEM analysis are presented in Fig. 3. In generator operation, for rated speed we have computed the air-gap flux density and the *emf*. The obtained results are very close to the analytical obtained ones. It can be observed that the *emf* is not very close to a sinusoidal wave form. Thus, in motor operation, even if the supplying current is a very smooth sinusoidal, the torque ripples are very high. A 44% torque ripples is obtained with the PMSM-9/54 topology.

The PMSM-23/51 was analyzed, too, on FEM. The numerical results are shown in Fig. 4. The air-gap flux density and the *emf* are plotted, from generator operation, at rated speed (420 r/min). The obtained results are very close to the analytical ones (see Table I). Concerning the *emf*, it can be observed that the wave form is very smooth and closed to a sinusoidal wave. This is the advantage of the fractioned type winding topology, which produces very smooth induced *emf*.

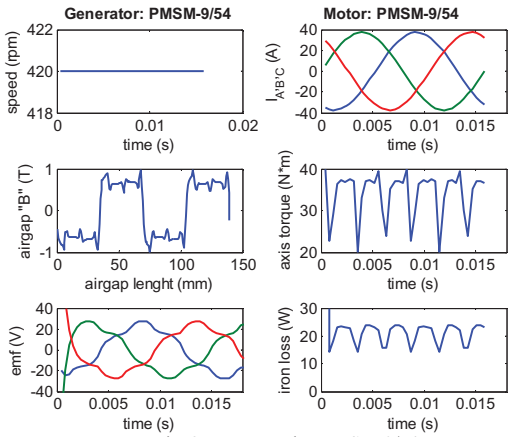

Fig. 3. FEM results: PMSM-9/54.

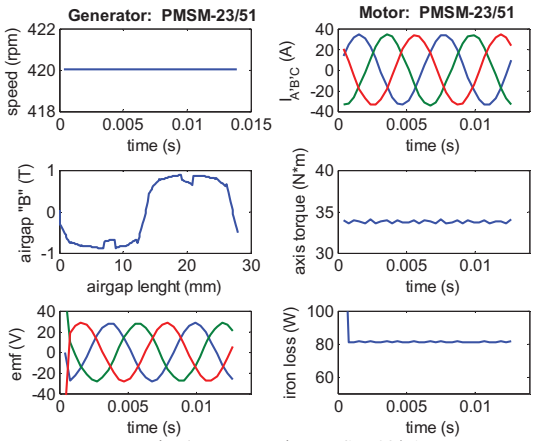

Fig. 4. FEM results: PMSM-23/51.

To see how this will affect the wave form, we have simulated the motor regime of the PMSM-23/51. With rated imposed current, the torque wave form is very smooth. The ripples are at 1.6 %. On the other hand, since the number of poles is very high, the supplying frequency is very important. This means that the iron loss are higher that for the PMSM-9/54. So, each topology has its own advantages and disadvantages. Because the PMSM-9/54 has reduced iron loss, we are trying to find a solution to reduce the torque ripples. Theoretically, skewing the stator core might produce a very smooth torque wave. For that, we have analyzed the PMSM-9/54 with the Flux/Skewed computation module.

The geometry of the PMSM-9/54 was drawn in 2D and after that we have considered an angle of incline of 1 slot (360/54=6.66°).

The effect on stator sheets incline, as well as the core flux density repartition, is shown in Fig. 5. Now, one can verify the torque repartition for the skewed machine, Fig. 6. The torque varies now between 33.3 and 35.78, meaning that the torque ripples are of 7.3%! This is an important decrease of torque ripples. This gain can be decisive while preparing the control of the PMSM.

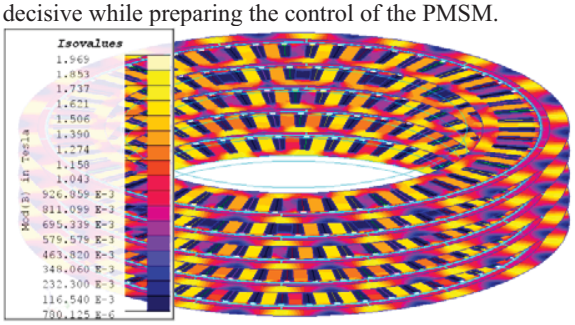

Fig. 5. Skewing the PMSM-9/54: flux density repartition.

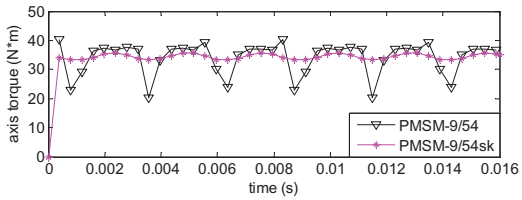

Fig. 6. PMSM-9/54, torque ripples: with or without skewing effect.

Of course, this skewing involves supplementary costs, but using reduced number of poles will reduce the frequency, and finally the iron loss.

IV. Simulating the Control of the Studied PMSM

One of the major problems of ac machines is that their inductive character reduces the power factor. The presence of PMs on the rotor surface involves high inductances values, thus reducing the energetic performances of the machine.

There are two ways to increase to power factor. The first way is to use a capacitor battery connected to the stator winding. This solution involves equipment and maintenance costs. The second way is to use an appropriate control strategy. This demands computational power of the control unit, but is less expensive and no maintenance is needed. The second solution will be employed here.

The unity power factor control strategy will be depicted further. From the phasor diagram of PMSM, Fig. 7, it is possible to rewrite the *d,q*-axis currents by imposing $\beta=(\delta-\varphi)$. Thus, the currents are $i_d=-I_s\cdot\sin(\beta)$ and $i_q=I_s\cdot\cos(\beta)$.

If one will choose the *q* axis as phase origin, the electric motor will operate to unity power factor ($\cos\varphi=1$) if $\beta=\delta$.

It is necessary to introduce the voltage equations:

$$U_d = R_{ph}\cdot i_d + L_d\cdot\frac{di_d}{dt} - \omega\cdot L_q\cdot i_q$$
$$U_q = R_{ph}\cdot i_q + L_q\cdot\frac{di_q}{dt} + \omega\cdot L_d\cdot i_d + \omega\cdot\psi_m \quad (1)$$

where L_d, L_q are the direct and quadrature inductances, ω is the electrical angular velocity, R_{ph} is the phase resistance and Ψ_m is the PM linkage flux. The internal angle can be expressed function of *d,q* axis voltages, $\tan\delta = -U_d/U_q$. Then, introducing the current expression, in stationary regime (derivate terms are suppressed), one will get:

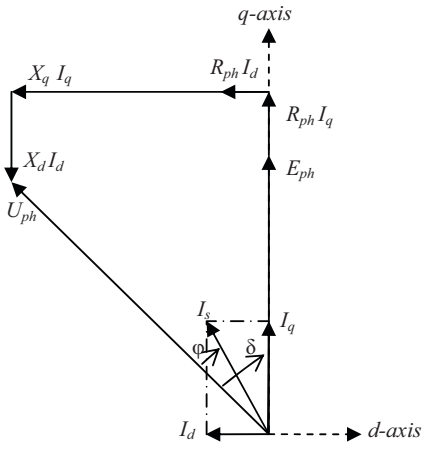

Fig. 7. Phasor diagram for PMSM in motor-load conditions.

$$\tan\delta = \frac{R_{ph}\cdot I_s\cdot\sin\beta + \omega\cdot L_q\cdot I_s\cdot\cos\beta}{R_{ph}\cdot I_s\cdot\cos\beta - \omega\cdot L_d\cdot I_s\cdot\sin\beta + \omega\cdot\psi_m} \quad (2)$$

Neglecting the phase resistance, the internal angle tangent becomes:

$$\tan\delta = \frac{\omega\cdot L_q\cdot I_s\cdot\cos\beta}{-\omega\cdot L_d\cdot I_s\cdot\sin\beta + \omega\cdot\psi_m} \quad (3)$$

For unity power factor, β=δ, the following equality appears:

$$\frac{\sin\beta}{\cos\beta} = \frac{\omega\cdot L_q\cdot I_s\cdot\cos\beta}{-\omega\cdot L_d\cdot I_s\cdot\sin\beta + \omega\cdot\psi_m} \quad (4)$$

After calculation, a second degree equation will be obtained, with the following solution:

$$\sin\beta = \frac{1\pm\sqrt{1-4\cdot\frac{L_d\cdot L_q\cdot I_s^2}{\psi_m}\cdot\left(1-\frac{L_q}{L_d}\right)}}{2\cdot\frac{L_d\cdot I_s}{\psi_m}\cdot\left(1-\frac{L_q}{L_d}\right)} \quad (5)$$

The mathematical model will be completed with the torque and motion equations:

$$T_e = p\cdot\left[\left(L_d - L_q\right)\cdot I_d\cdot I_q + \psi_m\cdot I_q\right] \quad (6)$$

$$\frac{d\Omega}{dt} = \frac{\left(T_e - B\cdot\Omega - T_l\right)}{J} \quad (7)$$

where B is the friction coefficient (measured in *N*m*s/rad*), Ω is the angular speed (measured in *rad/s*) and T_l is the load torque, J is the moment of inertia (measured in $kg*m^2$).

In order to prove the controllability at unity power factor, a vector control strategy is employed for the control of PMSM-23/51 [8]. The simulation results are presented in Fig. 8.

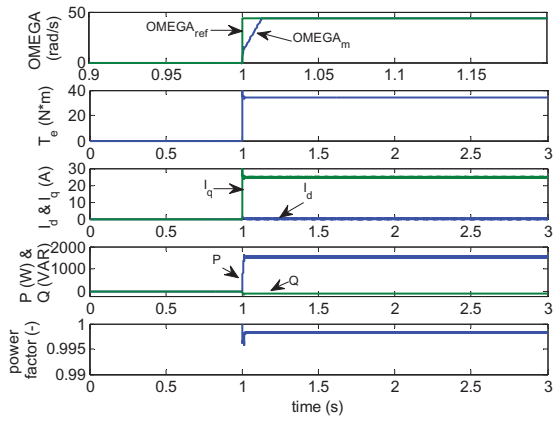

Fig. 8. Simulation results for controlling the PMSM-23/51 at unity power factor.

After 1 second the rated speed is imposed as reference (in *rad/sec*). The measured speed follows the reference one. At the same instant, the rated load torque of 34 *N*m* is considered. The absorbed electric power (corresponding to the active power *P*) and the reactive one, Q, as well as *d,q* axis currents are depicted also. The unity power-factor control strategy has been successfully employed since the simulated results show a power factor over 99%.

V. Conclusions

The paper presents the analytical and numerical results of a research study that concerns the use of PMSM in electric scooter application. Two motor configurations were analyzed, based on different winding configurations and poles/slots ratio. The analytical results have been validated by numerical ones. Also the skewing effect of the armature has been numerically evaluated, in order to decrease the torque ripples of one PMSM variant.

Finally, the major problem of ac machines, the reduced power factor, was solved through a proper control strategy. Through simulations, a unity power factor was obtained.

Acknowledgment

This paper was supported by the project "Development and support of multidisciplinary postdoctoral programmes in major technical areas of national strategy of Research - Development - Innovation" 4D-POSTDOC, contract no. POSDRU/89/1.5/S/52603, project co-funded by the European Social Fund through Sectoral Operational Programme Human Resources Development 2007-2013.

References

[1] Fuhs A.E., *Hybrid vehicle and the future of personal transportation*. CRC Press, 2009.

[2] Ehsani, M., Gao, Y., Gay, S.E., Emadi, A., *Hybrid Electric, and Fuel Cell Vehicles: Fundamentals, Theory, and Design*. CRC Press 2005.

[3] Vogel, C., *Build Your Own Electric Motorcycle*. McGraw-Hill Companies 2009.

[4] Ceraolo, M., Caleo, A., Campozella, P., Marcacci, M. *A parallel-hybrid drive-train for propulsion of a small scooter*, IEEE Transactions on Power Electronics, vol.21, no 3, pp.768-778, March 2006.

[5] Chenh-Hu, C., Ming-Yang, C., "Implementation of a highly reliable hybrid electric scooter drive", *IEEE Transactions on Industrial Electronics*, vol.54, no 5, pp.2462-2473, March 2007.

[6] http://www.icpe.ro/en/d/3/p/scooter.

[7] Pyrhonen, J., Jokinen, T. and Hrabovcova, V., *Design of Rotating Electrical Machines*. John Wiley & Sons, 2008.

[8] Fodorean, D., Djerdir, A., Miraoui, A., Viorel, I.A., *FOC and DTC Techniques for Controlling a Double Excited Synchronous Machine*, Proceedings of the IEEE International Electric Machines and Drives Conference.– IEMDC, Antalya, Turkey, 2007, pp. 1258-1263.